CRYSTAL GROWTH & DESIGN

Subscriber access provided by Brown University Library

Article

Tetrahedral Tetraphosphonic Acids. New Building Blocks in SupramolecularChemistry

Alexandra Schütrumpf, Erdo#an Kirpi, Aysun Bulut, Flavien L. Morel, Marco Ranocchiari,
Enno Lork, Yunus Zorlu, Simon Grabowsky, Gündo# Yücesan, and Jens Beckmann

Cryst. Growth Des., **Just Accepted Manuscript** • DOI: 10.1021/acs.cgd.5b00811 • Publication Date (Web): 21 Aug 2015

Downloaded from http://pubs.acs.org on August 23, 2015

Just Accepted

“Just Accepted” manuscripts have been peer-reviewed and accepted for publication. They are posted online prior to technical editing, formatting for publication and author proofing. The American Chemical Society provides “Just Accepted” as a free service to the research community to expedite the dissemination of scientific material as soon as possible after acceptance. “Just Accepted” manuscripts appear in full in PDF format accompanied by an HTML abstract. “Just Accepted” manuscripts have been fully peer reviewed, but should not be considered the official version of record. They are accessible to all readers and citable by the Digital Object Identifier (DOI®). “Just Accepted” is an optional service offered to authors. Therefore, the “Just Accepted” Web site may not include all articles that will be published in the journal. After a manuscript is technically edited and formatted, it will be removed from the “Just Accepted” Web site and published as an ASAP article. Note that technical editing may introduce minor changes to the manuscript text and/or graphics which could affect content, and all legal disclaimers and ethical guidelines that apply to the journal pertain. ACS cannot be held responsible for errors or consequences arising from the use of information contained in these “Just Accepted” manuscripts.

ACS Publications

Crystal Growth & Design is published by the American Chemical Society. 1155 Sixteenth Street N.W., Washington, DC 20036

Published by American Chemical Society. Copyright © American Chemical Society. However, no copyright claim is made to original U.S. Government works, or works produced by employees of any Commonwealth realm Crown government in the course of their duties.

Crystal Growth & Design - Full Article

Tetrahedral Tetraphosphonic Acids. New Building Blocks in Supramolecular Chemistry

Alexandra Schütrumpf,[a] Erdoğan Kirpi,[b] Aysun Bulut,[c] Flavien L. Morel,[d] Marco Ranocchiari,[e] Enno Lork,[a] Yunus Zorlu,[f] Simon Grabowsky,[a] Gündoğ Yücesan,[g*] Jens Beckmann[a*]

[a] *Institut für Anorganische Chemie und Kristallographie, Universität Bremen, Leobener Straße, 28359 Bremen, Germany.*

[b] *Department of Chemistry, Yildiz Technical University, Davutpasa Campus, Esenler, 34010 Istanbul, Turkey.*

[c] *Bölümü, Davutpaşa Cad. No.127, 34210 Esenler, İstanbul, Turkey.*

[d] *Department of Chemistry and Applied Biosciences, ETH Zürich, Vladimir-Prelog-Weg 1, 8093 Zürich, Switzerland.*

[e] *Laboratory for Catalysis and Sustainable Chemistry, Paul Scherrer Institut, 5232 Villigen, Switzerland.*

[f] *Gebze Technical University, Department of Chemistry, P. O. Box 141 Gebze, 41400 Kocaeli, Turkey.*

[g] *Yıldız Technical Üniversitesi Davutpaşa Kampüsü, Kimya-Metalürji Fakültesi, Biyomühendislik, Turkey.*

Received

Abstract

The structural characterization of tetraphenylmethane tetrakis-4-phosphonic acid (**4a**) and its closely related Si-analogue tetraphenylsilane tetrakis-4-phosphonic acid (**4b**) is reported. Crystals of **4a**, obtained by crystallization at 165°C from water under hydrothermal conditions, comprise a dense three-fold interpenetrated hydrogen-bonded network. Lower calculated density co-crystals **4b**·4 EtOH, attained by recrystallization from ethanol, give rise

---

[*] Correspondence to Jens Beckmann (E-mail: j.beckmann@uni-bremen.de) and Gündoğ Yücesan (E-mail: gyucesan@yildiz.edu.tr)

to a porous honeycomb network that shows no interpenetration. Isolated from the mother liquor the encapsulated ethanol is rapidly lost under ambient conditions leaving amorphous **4b**. While the amorphous **4b** is reasonably soluble in methanol, crystalline **4a** is virtually insoluble in common organic solvents.

Introduction

The construction of porous materials such as MOFs and COFs requires the judicious choice of rigid building blocks that contain functional groups suitable for metal coordination to form the desired organic-inorganic hybrid framework.[1-4] Particularly trigonal planar aromatic carboxylates provide structural rigidity and controllable design elements to produce isoreticular expansions with well-established secondary building units.[5-8] Most of the aromatic carboxylates with suitable sizes for MOF synthesis has been exploited to reach the optimum surface areas and gas adsorption properties. Although all these efforts to produce carboxylate-based MOFs have provided valuable insight into coordination chemistry, alternative bridging ligands with wider selection of adhesive functional groups such as, phosphonates[9-12] and arsenates[13] have been vastly neglected. The expansion of MOF research into different functional groups is required not only to produce novel MOFs with improved properties but also to address stability issues. Metal-organophosphonates form a well-known class of hybrid frameworks possessing wide range of applications including sorption, separation, optics and catalysis.[14-16] But their synthesis has been limited mostly to aliphatic diphoshonic acids and a comparatively few aromatic phosphonic acids.[17-47] Prominent examples include the trigonal building blocks 1,3,5-benzene tri(phosphonic acid),[34-40] 1,3,5-benzene tri(*p*-phenylphosphonic acid),[41-45] 1,3,5-triazine tri(phosphonic acid)[46] and 1,3,5-triazine tri(*p*-phenylphosphonic acid).[47] Phosphonates have tetrahedral RPO_3^{2-} structure with three oxygen atoms available for metal binding. The rich coordination modes of tetrahedral phosphonates on metal centers are expected to produce many new secondary building units with different transition elements.[48]

On the other hand, tetraphosphonates have multiple modes of tunable negative charges between 0 and -8, which is dependent on the reaction pH conditions. Therefore, they could initiate the formation of interesting metal oxidation states and novel metal clusters to balance the negative charges especially with transition metals possessing multiple oxidation states such as, vanadium, manganese and molybdenum etc. All these charge balance efforts could result in pH controlled tunable coordination chemistry producing interesting magnetic and catalytic properties.[49-52] MOFs constructed using the aromatic tetrahedral ligands are among the ones producing the highest porosities.[53-56] This is mostly due to the fact that the tetrahedral ligands open into three-dimensions with an angle of 109 degrees at the center of the ligand forming four trigonal pyramidal domes (Chart 1).

Chart 1. Tetrahedral building blocks based on tetraphenylmethane and -silane

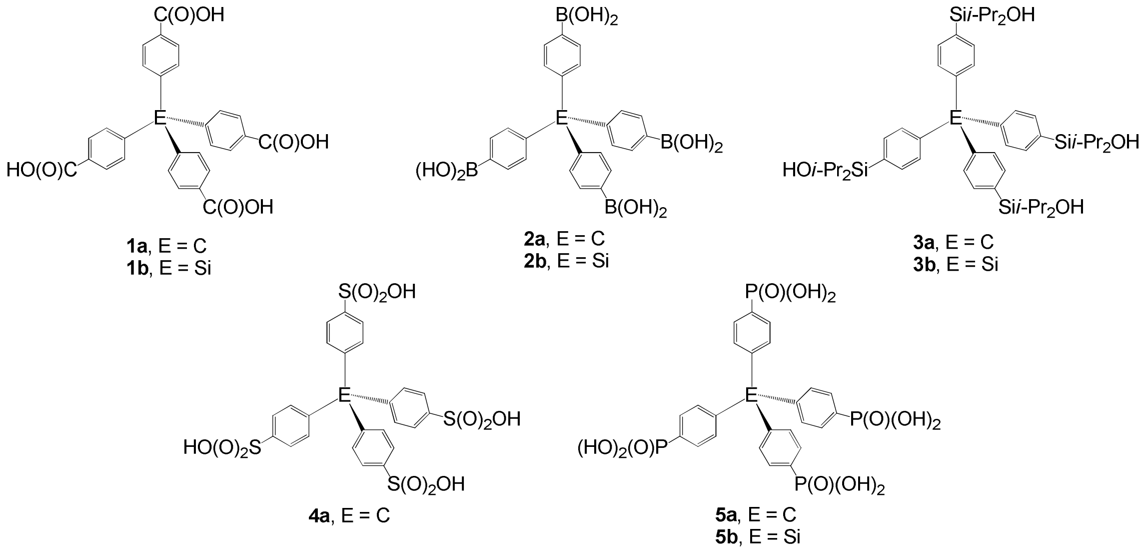

As the three-dimensional metal organic framework forms, these pyramidal domes are expected to expand into three-dimensional networks via metal centers to form the full cavities. The hydrophobic tetrahedral center is surrounded by hydrophilic adhesive functional groups providing that no metal oxides can penetrate into the tetrahedral cavities increasing the chances of obtaining void spaces.[57-60] On the other hand, planar aromatic ligands like 1,4-phenyldiphosphonic and 4,4'-biphenyldiphosphonic acids require special coordination modes on metal centers and solvent requirements to avoid π-stacking and pillared-layered organizations to form void spaces.[52] All these information suggests that when synthesized, tetrahedral phosphonate ligands would be very interesting linkers to produce more robust metal phosphonate frameworks providing diverse functions. Several tetrahedral building blocks based on tetraphenylmethane and -silane with different adhesive functional groups have already been reported already, which involve the carboxylic acids **1a** and **1b**,[61-65] the boronic acids **2a** and **2b,**[66] the silanols **3a** and **3b**[67] and the sulfonic acid **4a**[68] (Chart 1). We were interested to prepare the related arylphosphonic acids **5a** and **5b** to use them as building blocks in supramolecular chemistry. During the course of our work, the synthesis of tetraphenylmethane tetrakis-4-phosphonic acid (**5a**) was already reported by Zaręba and Zoń et al. In the same paper, the authors described crystals structures of corresponding pyridinium and ammonium phosphonates, however, no structural data of the free acid **5a** were disclosed.[69] Here we describe the synthesis of tetraphenylsilane tetrakis-4-phosphonic acid (**5b**) as well as the molecular and crystal structures of **5a** and **5b**.

Results and Discussion

The tetraphenylsilane tetrakis-4-phosphonic acid (**5b**) was prepared similarly as tetraphenylmethane tetrakis-4-phosphonic acid (**5a**)[69] in two synthetic steps starting from readily available tetrakis(4-bromophenyl)silane $(4\text{-BrC}_6\text{H}_4)_4\text{Si}$. The first step involves the Pd(0) catalyzed variation of the Arbuzov reaction using triisopropylphosphite as substrate. In this way, tetraphenylsilane tetrakis(4-diisopropyl phosphonate) (**6b**) was obtained after a chromatographic work-up and recrystallization in 35% yield as colorless high-melting crystals (Scheme 1). The liberation of the acid **5b** was achieved by the reaction of **6b** with conc.

hydrochloric acid. This simple acidic hydrolysis avoids the costly trimethylbromosilane, which has been used by Zaręba and Zoń et al.[69] Notably, the acidic hydrolysis procedure works also for **5a**. After recrystallisation from ethanol, **5a** and **5b** were obtained as ethanol solvates in 98% and 89% yield, respectively. Once isolated from the mother liquor the ethanol was rapidly lost leaving only amorphous materials.

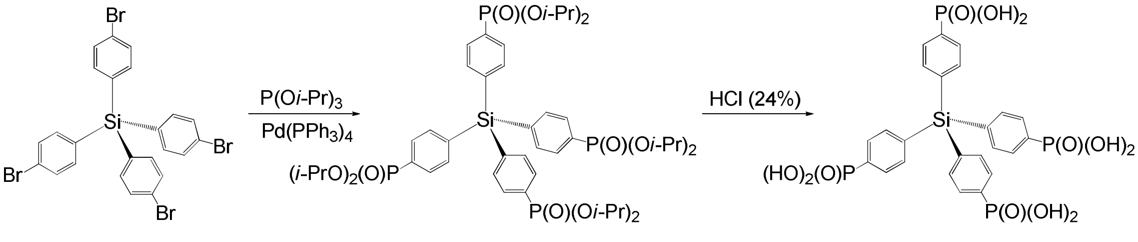

6b

5b

Scheme 1. Synthesis of tetraphenylsilane tetrakis-4-phosphonic acid (**5b**)

However, when covered by oil single crystals of **5b**·EtOH suitable for X-ray crystallography were obtained. High quality single crystals of **5a** were obtained in the form of rectangular plates by crystallization under hydrothermal conditions (165°C, autogeneous pressure) from water. Replacing the water by DMF using the same method between 150 and 200 °C produced the same crystals of **5a**. Under high pressure and temperature, the density of the crystals is anticipated to be higher. Consistently, the calculated density of **5a** (1.615 g cm^{-3}) is much higher than of **5b** (1.304 g cm^{-3}), respectively. The molecular structures of **5a** and **5b**·4 EtOH and a superimposed stick model are shown in Figure 1. The molecular structure of **6b** is shown in the ESI (Figure S1). Tetrahedral central atoms are only slightly distorted, which is reflected in C-C-C angles of **5a** (103.9(3)° and 112.3(2)°) and C-Si-C angles of **5b** (106.5(4)° and 111.0(2)° that differ only marginally from the ideal tetrahedral angle.

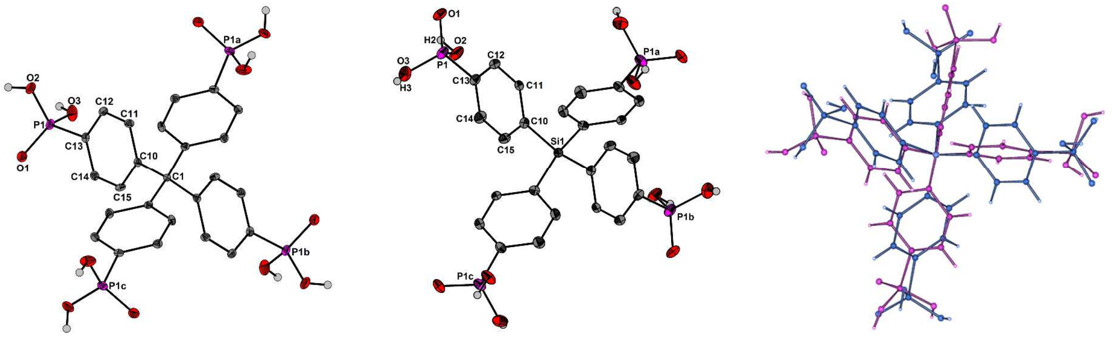

Figure 1. Molecular structures of **5a** (left) and **5b**·4 EtOH (middle) showing 30% probability ellipsoids and the crystallographic numbering scheme as well as superimposed stick models of **5a** and **5b** (right).

Together with the high rigidity of the phenyl rings both molecules possess very little conformational flexibility and consequently the molecular structure are very similar. Minor differences were observed in the alignment of the phenyl groups. In the crystal lattice individual molecules are associated by hydrogen bonding, which involves also of the solvated ethanol. The hydrogen-bond motifs of **5a** (left) and **5b**·4 EtOH are shown in Figure 2.

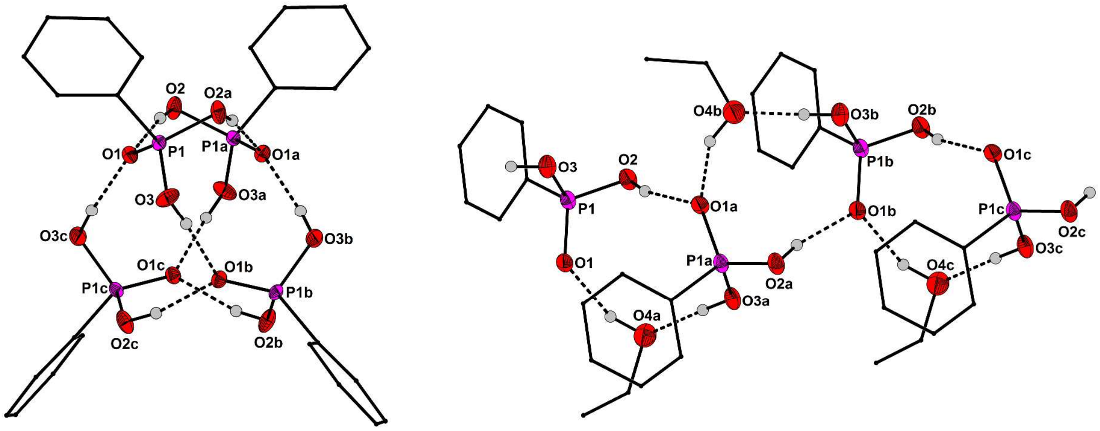

Figure 2. Hydrogen-bond motifs of **5a** (left) and **5b**·4 EtOH (right).

In **5a**, four phosphonate groups comprise a finite, 3D cage-like hydrogen-bonded network, whereas in **5b**·4 EtOH, a rather 2D infinite network propagates through the crystal lattice.

Both hydrogen-bonded motifs contain cyclic subunits that can be classified by the ternary graph set $R_3^3(10)$.[70] In all phosphonic acid moieties, the P=O groups accept two hydrogen atoms of OH groups giving to rise to bifurcated hydrogen-bridges typical for phosphonic acids.[71] While the P-OH groups act only as hydrogen bond donors, the ethanol molecules serves as both donor and acceptor of the hydrogen bridge. The short donor-acceptor distances of **5a** (O3a···O1c 2.579(5) Å) and **5b**·4 EtOH (O3a···O4a 2.538(1) Å, O2···O1a 2.563(1) Å) are indicative for strong hydrogen bonds and cooperativity.[71,72] Notably, in **5b**·4 EtOH there is also a weaker hydrogen bridge as evidenced by a longer donor-acceptor distances (O4a···O1 2.702(1) Å). In order to evaluate the importance of these hydrogen bonds for the crystal packing compared to other intermolecular forces, a Hirshfeld surface analysis was carried out. A Hirshfeld Surface (HS)[73] is the outer contour of the space which a molecule or an atom consumes in a crystalline environment. It can be compared to the van der Waals envelope which other molecules or atoms come into contact with when interactions are present. The directions and strengths of these interactions can be mapped onto the HSs using various descriptors such as d_{norm}.[74] This is a ratio encompassing the distances of any surface point to the nearby interior (d_i) and exterior atoms (d_e) and the van der Waals radii of the atoms.[74] Red colored regions in Figure 3a,b (i.e. negative values of d_{norm}) as well as flattened regions of the HS itself locally indicate the existence of close contacts. For both **5a** and **5b**, all of these contacts can be identified as classical hydrogen bonds. No other type of interaction is structurally directing according to the HS representations. Fingerprint plots[75] are a 2-dimensional projection of the d_{norm}-mapped HSs visualising contacts as d_i-d_e data points. Each data point represents the sum of the closest distances from any point on the HS to an internal and external atom, which can vary in length. Shortest contacts appear with distinct features such as spikes for O···H hydrogen bonds or peripheral spikes for C-H···π interactions, see Figures 3c,d.

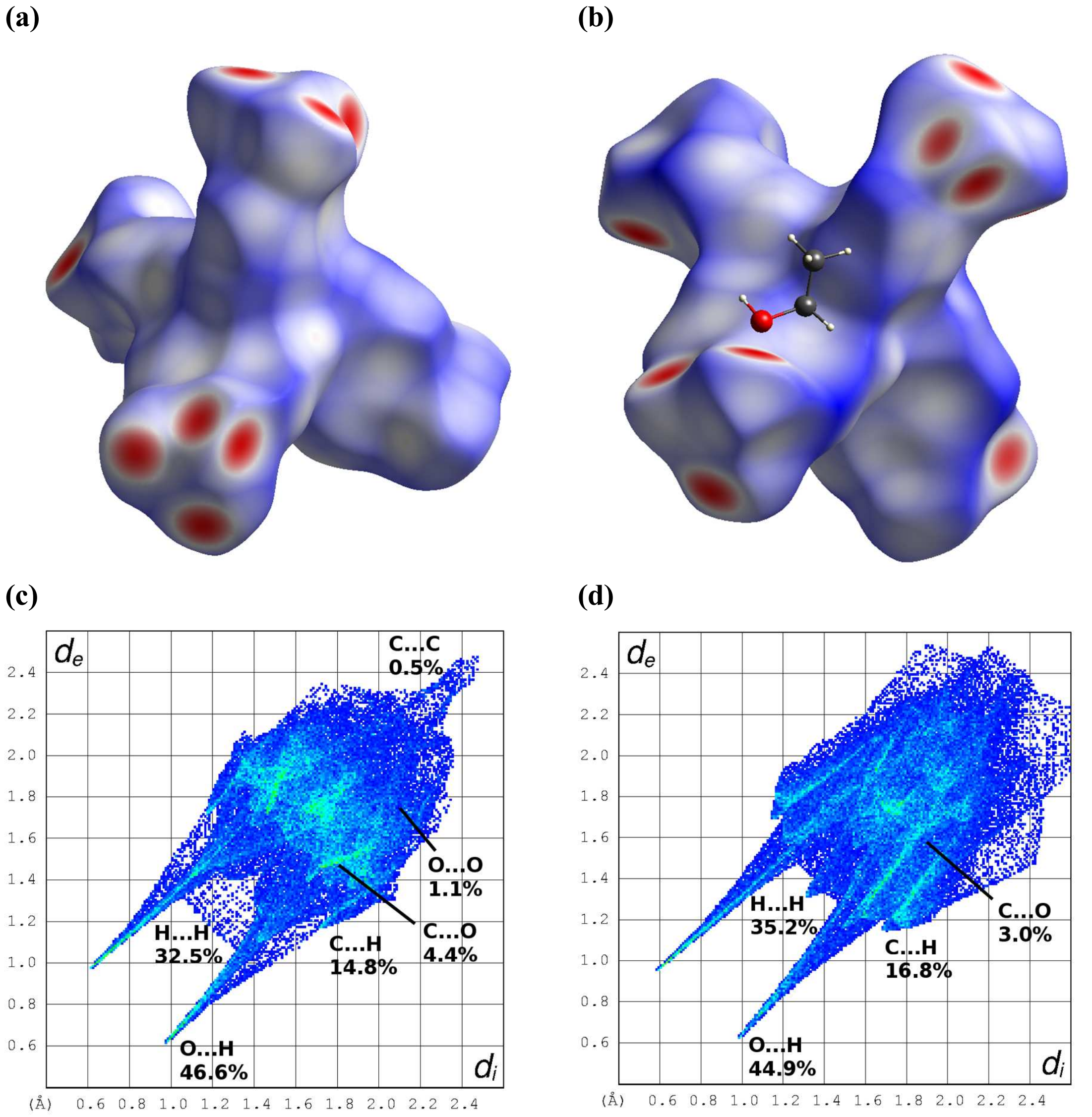

Figure 3. Hirshfeld Surfaces with d_{norm} mapped onto them for **5a** (a) and **5b** ·4 EtOH (b). Colour code = –0.821 (red) to 1.691 (blue). Fingerprint plots for **5a** (c) and **5b** ·4 EtOH (d) showing distinct features for characteristic short contacts (such as spikes) together with the overall percentage contribution of a contact type to the crystal packing. All pictures generated with the program *CrystalExplorer*.[76]

As an additional piece of information, the total percentage contribution of each contact type to the crystal packing is added to these Figures. Both compounds have very similar fingerprint plots, dominated by hydrogen bonding in terms of both the characteristic spikes and the total contribution (46.6% for **5a**, 44.9% for **5b**). Dispersive H···H contacts follow in terms of the contributions (32.5% for **5a**, 35.2% for **5b**). In contrast C···H contacts that represent C-H···π interactions are neither dominant in terms of the features and the contributions (14.8% and 16.8%). All other contact types (C···O, C···C, O···O) are below 5%. More detailed fingerprint information is given in the Supporting information. As anticipated from the very different calculated densities, the crystal structures of **5a** and **5b**·4 EtOH are also significantly different. The topological analysis unraveling the connectivity patterns of the hydrogen bonded networks are shown in Figure 4.

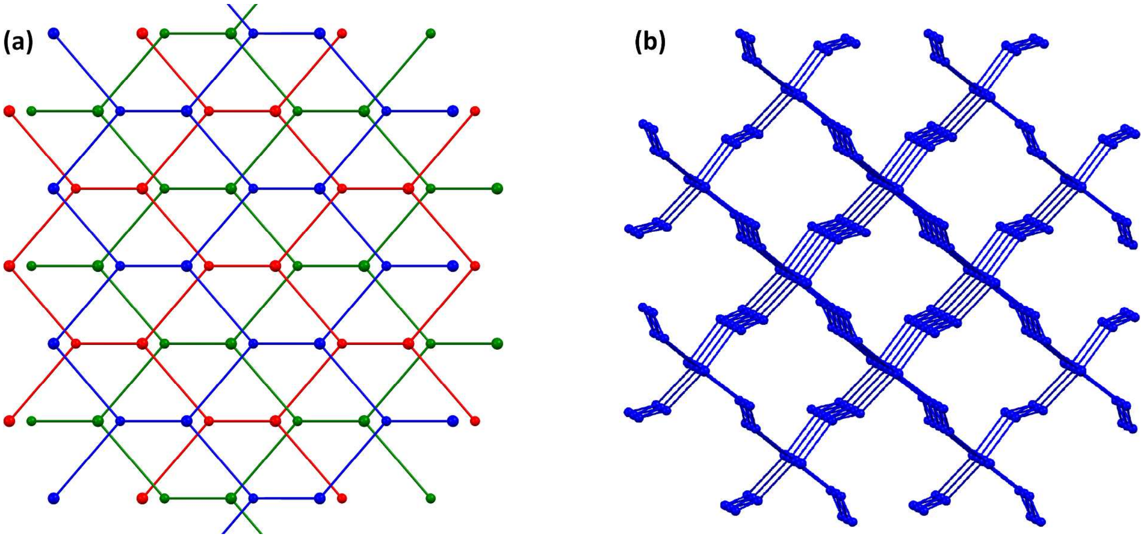

Figure 4. (a) View of the 3-fold interpenetrating hydrogen bonded networks of **5a**. The three networks are presented in green, blue, and red. (b) View of the single 3D hydrogen bonded network of **5b**.

The simplified network of **5a** comprises a three-fold interpenetrating array similarly as present in textile fabrics, whereas **5b** possess honeycomb porous networks without any interpenetration.[77-79] The inside of these pores is filled by the ethyl groups of the solvated ethanol. The high volatility of the ethanol upon isolation from the mother liquor raises the question the stability of the remaining network and the void space. Calculation of the void space of **5b**·4 EtOH using the crystal data and *Crystal Explorer*[76] (iso value 0.0003) reveals that only 1.5% of the cell volume was accessible by small gas molecules.[80] Under the assumption that the remaining network stayed intact, the ethanol was hypothetically removed from the crystal data (by deleting the coordinates from the cif file). In this case the assessable void space increased to 28.4%. To verify the validity of the assumption a bulk sample of **5b**·4 EtOH was dried in high vacuum at room temperature until the weight was constant. The amorphous sample obtained, hereafter referred to as **5b**, remains soluble in methanol. This noteworthy as crystals of **5a** prepared under hydrothermal conditions are virtually insoluble, presumably due the high lattice energy associated with the three-fold interpenetrating network. The ^{31}P NMR spectrum (D$_4$-methanol) of **5b** shows a single resonance at $\delta = 16.5$ ppm. Consistent with the loss of crystallinity, an X-ray powder diffractogram exhibits no reflections for **5b**, which suggests that the remaining hydrogen-bonded network collapsed when the ethanol was removed. This was also confirmed by measuring the BET surface area, which showed virtually no N_2 physisorption of **5b** at 77K. The amorphous **5b** was further characterized by ^{31}P MAS NMR spectroscopy and DTA analysis. The ^{31}P MAS NMR spectrum of **5b** shows a main signal at $\delta_{iso} = 24.5$ ppm and minor intense signals at $\delta_{iso} = 38.2$, 18.5 and 0.2 ppm (see ESI for the spectrum). The number of signals is attributed to the different local environments of the phosphorous atoms. The signals at $\delta_{iso} = 24.5$ and 18.5 ppm were tentatively assigned to phosphonate groups being involved in different hydrogen-bond motifs. The signal at $\delta_{iso} = 38.2$ might be due to a phosphonate group in which one or both OH groups are not-hydrogen bonded. The small signal at $\delta_{iso} = 0.2$ ppm might even belong to phosphonate that underwent condensation (see below). The DTA analysis shows mass loss of about 10% up to 300°C, most likely water that formed during the condensation of phosphonate groups. When a bulk sample of **5b** was heated for 14 h at 280°C, a colourless amorphous sample, hereafter named **5b**' was obtained and water was detected in the cooling trap. In contrast to **5b**, the heated sample **5b**' was virtually insoluble in methanol or other solvents. The ^{31}P MAS NMR spectrum of **5b**' gave rise to a main signal at $\delta_{iso} = -1.3$ ppm and two minor intense signals at 6.5 and –12.6 ppm. The poor solubility and the high-field shift of the ^{31}P MAS NMR resonances suggest that the (partial) condensation of P-OH groups into P-O-P linkages took place. Measurement of the BET surface area confirmed that **5b**' also lacks any porosity. The DTA analysis of **5b** above 300°C indicates complete thermal degradation of the material in two mass loss incidents from 300 to 550°C (40%) and from 550 to 800°C (20%).

Conclusions

Besides the very recently reported tetraphenylmethane tetrakis-4-phosphonic acid (**5a**),[69] the closely related Si-analogue tetraphenylsilane tetrakis-4-phosphonic acid (**5b**) was prepared in two synthetic steps. Although the molecular structures of **5a** and **5b** are very similar, the crystal structures are significantly different, which can be related to the way the crystals were grown. Highly dense crystals of **5a** were obtained by crystallization from water at 165°C under hydrothermal conditions. The crystal structure of **5a** features a three-folded hydrogen-bonded network, which explains the virtual insolubility in methanol and other organic solvents. Recrystallization from ethanol under normal pressure afforded lower density co-crystals with the solvent, **5b**·4 EtOH, the crystal structure of which reveals a porous honeycomb network that lacks interpenetration. Once isolated from the mother liquor, the ethanol molecules, situated partly in the voids defuse out of the crystal lattice leaving amorphous **5b** still being soluble in methanol. Heating **5b** at temperatures nearly 300°C proceeds with condensation of the P-OH groups to give an insoluble cross-linked material with P-O-P linkages. Due to conformational rigidity, **5a** and **5b** hold great potential as tetrahedral building blocks for the preparation of metal organic frameworks (MOFs), which is actively being pursued in our laboratories.

Associated Content

Supporting Information

Crystallographic data files in CIF format, experimental procedures, crystal and refinement details, Fingerprints for the separate intermolecular forces, thermogravimetric analysis, solid-state ^{31}P NMR spectroscopy, Nitrogen physisorption, additional references. This material is available free of charge via the internet at http://pubs.acs.org.

Author Information

Corresponding Authors

* J.B. E-mail: j.beckmann@uni-bremen.de)

* G.Y. E-mail: gyucesan@yildiz.edu.tr

Notes

The authors declare no competing financial interest

Acknowledgement

Financial support by the Deutsche Forschungsgemeinschaft (DFG) within the Emmy Noether scheme GR4451/1-1 and the Türkiye Bilimsel ve Teknolojik Araştırma Kurumu (TÜBİTAK 212T060) is gratefully acknowledged.

Dedication

Dedicated to Professor Derek Woollins on the occasion of his 60th birthday

References

[1] Desiraju, G. R. In *Crystal Engineering: The Design of Organic Solids*; Elsevier: Amsterdam, 1989.

[2] Vögtle, F. In *Supramolecular Chemistry*; Wiley: Chichester, 1991.

[3] Lehn, J.-M. In *Supramolecular Chemistry: Concepts and Perspectives*; VCH: New York, 1995.

[4] Lehn, J.-M. In *Comprehensive Supramolecular Chemistry*; Pergamon: New York, 1996.

[5] Furukawa, H.; Cordova, K. E.; O'Keeffe, M.; Yaghi, O. M. *Science* **2013**, *341*, 974-988.

[6] Furukawa, H.; Ko, N.; Go, Y. B.; Aratani, N.; Choi, S. B.; Choi, E.; Yazaydin, A. Ö.; Snurr, R. Q.; O'Keeffe, M.; Kim, J.; Yaghi, O. M. *Science* **2010**, *329*, 424-428.

[7] Guillerm, V.; Kim, D.; Eubank, J. F.; Luebke, R.; Liu, X.; Adil, K.; Lah, M. S.; Eddaoudi, M. *Chem. Soc. Rev.*, **2014**, *43*, 6141-6172 and references therein.

[8] Yaghi, O. M.; O'Keeffe, M.; Ockwig, N. W.; Chae, H. K.; Eddaoudi, M.; Kim, J. *Nature* **2003**, *423*, 705-714.

[9] Clearfield, A. In *Design of New Materials*; eds. Cocke, D. L., Clearfield, A. Plenum: New York, 1986; p 121.

[10] Clearfield, A. *Solvent Extr. Ion Exch.*, **2000**, *18*, 655-678.

[11] Byrd, H.; Clearfield, A.; Poojay, D. M.; Reis, K. P.; Thompson, M. E. *Chem. Mater.* **1996**, *8*, 2239-2246.

[12] Konar, S.; Zoñ, J.; Prosvirin, A. V.; Dunbar, K. R.; Clearfield, A. *Inorg. Chem*. **2007**, *46*, 5229-5236 and references therein.

[13] Burkholder, E.; Wright, S.; Golub, V.; O'Connor, C. J.; Zubieta, J. *Inorg. Chem.* **2003**, *42*, 7460-7471.

[14] Kevin J.; Gagnon, K. J.; Perry, H. P.; Clearfield, A. *Chem. Rev*. **2012**, *112*, 1034-1054.

[15] Luebke, R.; Weseliński, L. J.; Belmabkhout, Y.; Chen, Z.; Wojtas, Ł.; Eddaoudi, M. *Cryst. Growth Des*. **2014**, *14*, 414-418.

[16] Yiing, S.-M.; Mao, J.-G. *Cryst. Growth Des*. **2006**, *6*, 964-968.

[17] Clearfield, A.; Wang, Z. *J. Chem. Soc., Dalton Trans*. **2002**, 2937-2947.

[18] Finn, R. C.; Zubieta, J.; Haushalter, R. C. *Crystal Chemistry of Organically Templated Vanadium Phosphates and Organophosphonates*; John Wiley & Sons, Inc.: New York, **2003**; p 421.

[19] Fu, R.-B.; Wu, X.-T.; Hu, S.-M.; Zhang, J.-J.; Fu, Z.-Y.; Du, W.-X. *Polyhedron* **2003**, *22*, 2739-2744.

[20] Merrill, C. A.; Cheetham, A. K. *Inorg. Chem*. **2005**, *44*, 5273-5277.

[21] Merrill, C. A.; Cheetham, A. K. *Inorg. Chem*. **2007**, *46*, 278-284.

[22] Ouellette, W.; Yu, M. H.; O’Connor, C. J.; Zubieta, J. *Inorg. Chem*. **2006**, *45*, 3224-3229.

[23] Ouellette, W.; Yu, M. H.; O’Connor, C. J.; Zubieta, *J. Inorg. Chem*. **2006**, 45, 7628-7641.

[24] Yücesan, G.; Golub, V.; O’Connor C. J.; Zubieta, J. *Dalton Trans*. **2005**, 2241-2251.

[25] Shimizu, G. K. H.; Vaidhyanathan, R.; Taylor, J. M. *Chem. Soc. Rev*., **2009**, *38*, 1430-1449.

[26] Clearfield, A. *Curr. Opin. Solid State Mater. Sci*. **1996**, *1*, 268-278.

[27] Clearfield, A. *Curr. Opin. Solid State Mater. Sci*. **2002**, *6*, 495-506.

[28] Clearfield, A.; Wang, Z. *J. Chem. Soc., Dalton Trans*. **2002**, 2937-2047.

[29] Vioux, A.; Le Bideau, J.; Mutin, P. H.; Leclercq, D. *Top. Curr. Chem*. **2004**, *232*, 145-174.

[30] Maeda, K. *Micropor. Mesopor. Mat.* **2004**, *73*, 47-55.

[31] Mosby, B. M.; Díaz, A.; Clearfield, A. *Dalton Trans*., **2014**, *43*, 10328-10339.

[32] Białek, M. J.; Janczak, J.; Zoñ, J. *CrystEngComm*, **2013**, *15*, 390-399.

[33] Białek, M. J.; Zaręba, J. K.; Janczak J.; Zoñ, J. *Cryst. Growth Des*. **2013**, *13*, 4039-4050.

[34] Mehring, M. *Eur. J. Inorg. Chem*. **2004**, 3240-3246.

[35] Kong, D. ; Clearfield, A. ; Zoń, *J. Crystal Growth Des*. **2005**, *5*, 1767-1773.

[36] Kong, D.; Zoñ, J.; McBee, J.; Clearfield, A. *Inorg. Chem*. **2006**, *45*, 977-986.

[37] Hix, G. B. ; Caignaert, V. ; Rueff, J.-M.; Le Pluart, L. ; Warren, J. E. ; Jaffrès, P.-A. *Crystal Growth Des*. **2007**, *7*, 208-211.

[38] Kong, D. ; Clearfield, A. ; Zoñ, J. *Crystal Growth Des*. **2008**, *8*, 2892-2898.

[39] Taylor, J. M. ; Mah, R. K. ; Moudrakovski, I. L. ; Ratcliffe, C. I. ; Vaidhyanathan, R. ; Shimizu, G. K. H. *J. Am. Chem. Soc*. **2010**, *132*, 14055-14057.

[40] Pramanik, M. ; Bhaumik, A. *Chem. Eur. J*. **2013**, *19*, 8507-8514.

[41] Beckmann, J.; Rüttinger, R.; Schwich, T. *Cryst. Growth Des*. **2008**, *8*, 3271-3276.

[42] Vaidhyanathan, R. ; Mahmoudkhani, A. H. ; Shimizu, G. K. H. *Can. J. Chem*. **2009**, *87*, 247-253.

[43] Ouellette, W.; Wang, G.; Liu, H.; Yee, G. T.; O'Connor, C. J.; Zubieta, J. *Inorg. Chem*. **2009**, *48*, 953-963.

[44] Mah, R. K.; Lui, M. W.; Shimizu, G. K. H. *Inorg. Chem*. **2013**, *52*, 7311-7313.

[45] Taddei, M.; Costantino, F.; Vivani, R.; Sabatini, S.; Lim, S.-H. Cohen, S. M. *Chem. Commun*. **2014**, *50*, 5737-5740.

[46] Maxim, C. ; Matni, A. ; Geoffroy, M. ; Andruh, M.; Hearns, N.G.R. Clérac, R. ; Avarvari, N. *New J. Chem*. **2010**, *34*, 2319-2327.

[47] Hermer, N.; Stock, N. *Dalton Trans*. **2015**, *44*, 3720-3723.

[48] Sahoo, D.; Suriyanarayanan, R.; Chandrasekhar V. *Dalton Trans.* **2014**, 43, 10898-10909.

[49] Meada, K. *Micropor. Mesopor. Mat*. **2004**, *73*, 47-55.

[50] Du, Z.-Y.; Xu, H.-B.; Mao, J.-G. *Inorg. Chem*. **2006**, *45*, 6424-6430.

[51] Kahn, O. *Molecular Magnetizm*; VCH:New York, 1993.

[52] Clearfield, A.; Demadis K. *Metal Phosphonate Chemistry: From Synthesis to Applications*; RSC Publishing:Cambridge, 2012.

[53] Zhang, Y.-B.; Su, J.; Furukawa, H.; Yun, Y.; Gándara, F.; Duong, A.; Zou, X.; Yaghi, O. M. *J. Am. Chem. Soc*. **2013**, *135*, 16336-16339.

[54] Li, M.; Li, D.; O'Keeffe, M.; Yaghi, O. M. *Chem. Rev*. **2014**, *114*, 1343-1370.

[55] Dinca, M.; Dailly, A.; Long, J. R. *Chem. Eur. J*. **2008**, *14*, 10280-10285.

[56] Ren; H.; Ben, T.; Wang, E.; Jing, X.; Xue, M.; Liu, B.; Cui, Y.; Qiua, S.; Zhu, G. *Chem. Commun*. **2010**, *46*, 291-293.

[57] Vasylyev, M.; Neumann, R. *Chem. Mater*. **2006**, *18*, 2781-2783.

[58] Vasylyev, M.; Wachtel, E. J.; Popovitz-Biro, R.; Neumann, R. *Chem. Eur. J*. **2006**, *12*, 3507-3514.

[59] Taylor, J. M.; Mahmoudkhani, A. H.; Shimizu, G. K. H. *Angew. Chem. Int. Ed*. **2007**, *46*, 795-798.

[60] Jones, K. M. E.; Mahmoudkhani, A. H.; Chandler, B. D.; Shimizu, G. K. H. *CrystEngComm* **2006**, *8*, 303-305.

[61] Lambert, J. B.; Liu, Z.; Liu, C. *Organometallics* **2008**, *27*, 1464-1469.

[62] Davies, R. P.; Less, R. J.; Lickiss, P. D.; Robertson, K; White, A. J.; P. *Inorg. Chem*. **2008**, *47*, 9958-9964.

[63] Davies, R. P.; Less, R.; Lickiss, P. D.; Robertson, K.; White, A. J. P. *Organometallics* **2010**, *10*, 4571-4581.

[64] Mandic, S.; Healey, M. R.; Gotthardt, J. M.; Alley, K. G. Gable, R. W.; Ritchie, C.; Boskovic, C. *Eur. J. Inorg. Chem*. **2013**, 1631-1634.

[65] Lee, J. H.; Moon, B.; Kim, T. K.; Jeoung, S.; Moon, H. R. *Dalton Trans*. **2015**, **DOI:** 10.1039/C5DT00690B.

[66] Fournier, J.-H.; Maris, T., Wuest, J. D.; Guo, W.; Galoppini, E. *J. Amer. Chem. Soc*. **2003**, *125*, 1002-1006.

[67] Kawakami, Y.; Sakuma, Y.; Wakuda, T.; Nakai, T.; Shirasaka, M.; Kabe, Y. *Organometallics* **2010**, *29*, 3281-3288.

[68] Sarma, B.; Nangia, A. *CrystEngComm.* **2007**, *9*, 628-631.

[69] Zareba, J. K.; Bialek, M. J.; Janczak, J.; Zoñ, J.; Dobosz, A. *Crystal Growth Des*. **2014**, *14*, 6143-6153.

[70] Bernstein, J.; Davies, R. E.; Shimoni, L.; Chang, N.-L. *Angew. Chem. Int. Ed*. **1995**, *34*, 1555-1573.

[71] Mehring, M.; Schürmann, M.; Ludwig, R. *Chem. Eur. J*. **2003**, *9*, 838-849.

[72] Steiner, T. *Angew. Chem. Int. Ed*. **2002**, *41*, 49-76.

[73] Spackman, M. A.; Byrom, P. G. *Chem. Phys. Lett.*, **1997**, *267*, 215-220.

[74] McKinnon, J. J.; Jayatilaka, D.; Spackman, M. A. *Chem. Commun.* **2007**, 3814-3816.

[75] Spackman, M. A.; McKinnon, J. J. *CrystEngComm.* **2002**, *4*, 378-392.

[76] CrystalExplorer (Version 3.1), Wolff, S.K.; Grimwood, D.J.; McKinnon, J.J.; Turner, M.J.; Jayatilaka, D.; Spackman, M.A. University of Western Australia, **2012**.

[77] Blatov, V. A. TOPOS 4.0 Professional, Commission on Crystallographic Computing, IUCr, 2006.

[78] Alexandrov, E. V.; Blatov, V. A.; Kochetkov, A. V.; Proserpio, D. M. *CrystEngComm* **2011**, *13*, 3947-3958.

[79] Blatov, V. A. *Struct. Chem*. **2012**, *23*, 955-963.

[80] Turner, M. J.; McKinnon, J. J.; Jayatilaka, D.; Spackman, M. A. *CrystEngComm.* **2011**, *13*, 1804-1813.

For table of contents use only

Tetrahedral Tetraphosphonic Acids. New Building Blocks in Supramolecular Chemistry

Alexandra Schütrumpf, Erdoğan Kirpi, Aysun Bulut, Flavien L. Morel, Marco Ranocchiari,

Enno Lork, Yunus Zorlu, Simon Grabowsky, Gündoğ Yücesan, Jens Beckmann

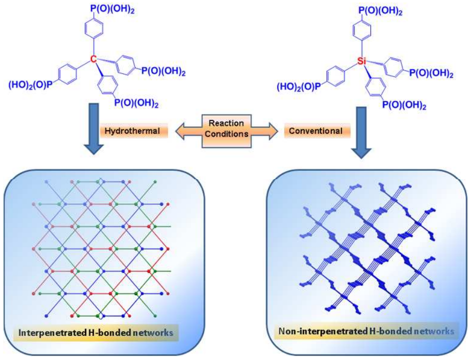

Tetraphenylmethane tetrakis-4-phosphonic acid crystallized under hydrothermal conditions provided a dense three-fold interpenetrated hydrogen-bonded network, whereas the closely related tetraphenylsilane tetrakis-4-phosphonic acid crystallized from ethanol to give rise to a porous honeycomb network that shows no interpenetration.